

FIBRE-TAPER DEVICES

F.P. Payne, C.D. Hussey,
Department of Electronics and Information Engineering
Southampton University

Abstract

In this paper I will review recent work at Southampton on tapered single mode optical fibre devices. In particular I will describe our recent work on single mode beam expanders and fused fibre couplers. It is well known that a gap of up to 100 μm in a single mode fibre results in about 1dB loss. By tapering the fibre so that the field expands into an LP_{01} cladding mode with increased spot size it is possible to introduce a larger gap of about one mm. This will allow the insertion of small electro-optic devices, such as a liquid crystal cell. By overjacketing the fibre with a silica capillary, or combination of Vycor and silica capillaries it should be possible to achieve a beam diameter of several hundred microns. This would allow a gap of about 1 cm and this would allow the insertion of a very wide range of optical devices, such as acousto optic modulators. Considerable progress has been made recently in the fabrication and analysis of long fused-taper 4-port directional couplers. This has resulted in several important devices, including polarization beam splitters, wavelength division multiplexers, optical fibre filters, and wavelength selective ring resonators.

TAPERS IN SINGLE MODE FIBRES

(i) Physical Properties

To modulate or switch the signal in a single mode optical fibre it is necessary to be able to interact with the electromagnetic field in the fibre core. One method of achieving this is by polishing away the cladding until it is within about a micron of the core. It is then possible to interact with the field in the core by varying the refractive index adjacent to the polished surface or by placing two polished fibres in contact to form an evanescent coupler. The main disadvantage of this method is that it is expensive and time consuming.

A simpler and much less expensive technique of gaining access to the field is by tapering. A single mode taper is made by fusing and pulling a single mode fibre of about 100 μm initial diameter in a small oxy-butane flame. A typical taper has a diameter of 10-20 μm at its narrowest point and a total taper length of 10-20 mm. The tapering has a significant effect on the optical field as it propagates along the fibre and the evolution of the field along a taper is shown schematically in Fig. 1. Initially the field is guided by the core. As the core diameter decreases the field spreads out, its spot size increasing as¹

$$\omega_0 = a \left(0.65 + \frac{1.619}{V^{3/2}} + \frac{2.879}{V^6} \right) \quad \dots(1)$$

Eventually, a point is reached when the field is no longer guided by the core but is effectively guided by a waveguide consisting of the cladding and surrounding medium. This cladding waveguide is highly multimoded and if the taper rate is large enough coupling to higher order modes will occur, and this will result in power loss from the output of the taper. The condition for a taper to remain adiabatic is^{2,3}

$$\frac{d\delta}{dz} \ll \frac{\delta}{z_b}, \quad z_b = \frac{2\pi}{|\beta_1 - \beta_2|} \quad (2)$$

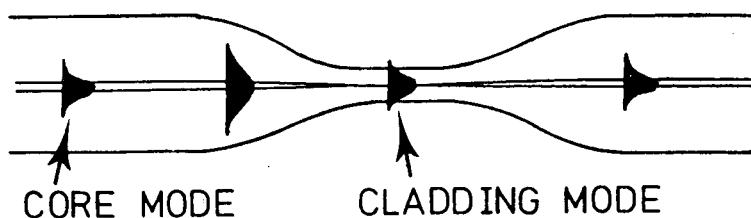


Fig. 1. Field evolution through a single mode adiabatic taper.

Here, β_1 and β_2 are the propagation constants of the LP_{01} mode and the LP_{02} cladding mode. A taper satisfying this condition will suffer negligible loss through mode coupling, and is a condition that is easily achieved in tapers made from matched cladding single mode fibres.

The power transmitted through an adiabatic taper decreases sharply when the refractive index of the external medium equals that of the silica cladding. This behaviour is demonstrated in Fig 2⁴ for a taper with a taper ratio (initial diameter/minimum diameter) of 5. By surrounding the taper with an electro-optic material such as a liquid crystal it should be possible to construct a simple on-off optical switch.

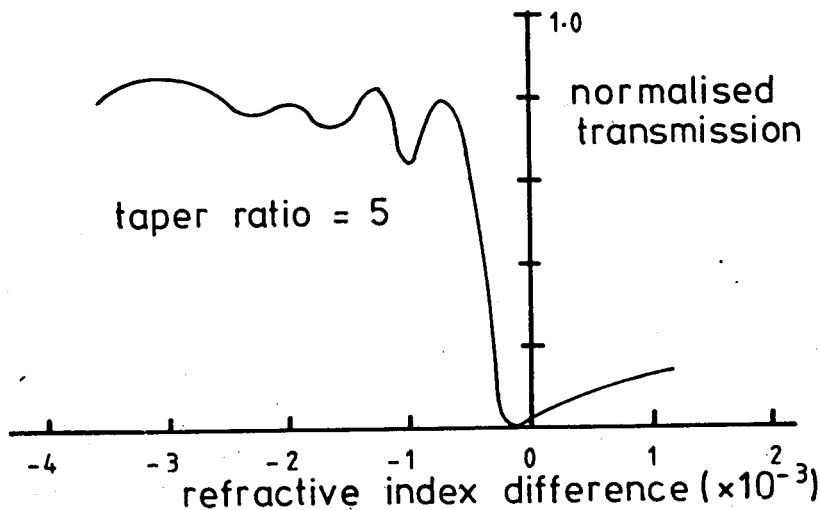


Fig. 2. Transmission characteristics of an adiabatic taper.

(ii) *Beam Expanders and Fibre-Gap Devices*

A gap cut in a single mode fibre, Fig 3, results in a transmission loss of $-10 \log_{10} T$, where

$$T = \frac{4(1 + z^2/z_0^2)}{(2 + z^2/z_0^2)^2} \tag{3}$$

$$\text{and } z_0 = \frac{\pi \omega_0^2 \eta}{\lambda}$$

The spot size of the mode as it leaves the fibre is ω_0 and η is the refractive index of the intervening material. Equation (3) is based on standard formulae for the diffraction of Gaussian beams⁵. A standard single mode fibre has a spot size of 2–3 μm and a gap of 150 μm results in about 3dB loss in an index matching medium. This gap size is rather small for the insertion of an electro-optic device such as a liquid crystal cell or acousto-optic modulator. From equation (3) we see that the gap size for a given loss increases as the square of the spot size and a moderate increase in spot size to about 9 μm will result in a gap of 1–2 mm, for a 3dB loss. The simplest method of achieving this, which avoids the use of lenses, is to adiabatically taper a single mode fibre to a diameter of about 20 μm . If the taper is cleaved at this point the field will

consist of an LP_{01} cladding mode with a spot size $8 - 9 \mu\text{m}$ and a 3dB gap of about 1.5 mm, Fig. 4. Unfortunately the tapered end is extremely fragile and difficult to cleave accurately. The expanded beam is also very sensitive to perturbations of the air cladding boundary. For these reasons a more practical device has been investigated where a 'Vycor' capillary sleeve of about $500 \mu\text{m}$ diameter has been placed around the fibre before tapering. The combined fibre and capillary were then tapered and the taper cleaved at a diameter of about $100 \mu\text{m}$, Fig. 5. Vycor has a slightly lower refractive index than silica ($\Delta n \approx .004$) and the fibre cladding mode is now guided by the boundary of the $20 \mu\text{m}$ final fibre and the Vycor. The expanded mode has a spot size of about $8 \mu\text{m}$ (Fig. 6) and is well protected by the easily cleaved Vycor jacket. The evolution of the spot size from core to cladding mode is clearly seen in Fig. 6.

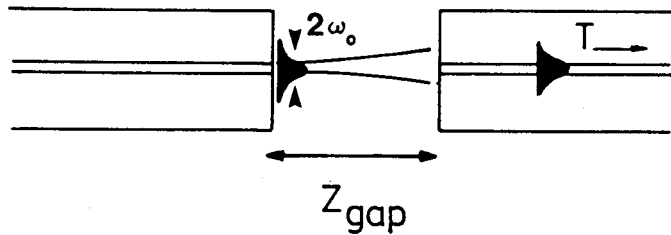


Fig. 3. Transmission across a gap in a single mode fibre.

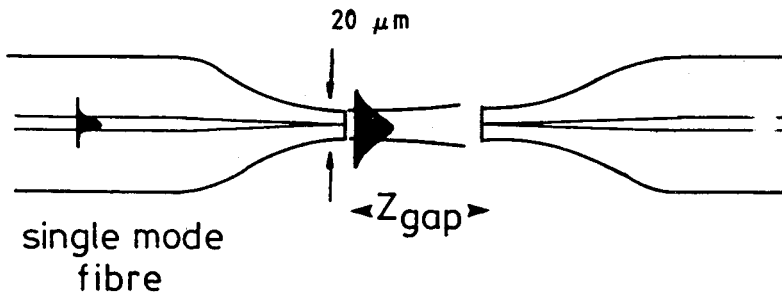


Fig. 4. Taper beam expansion to increase fibre gap size.

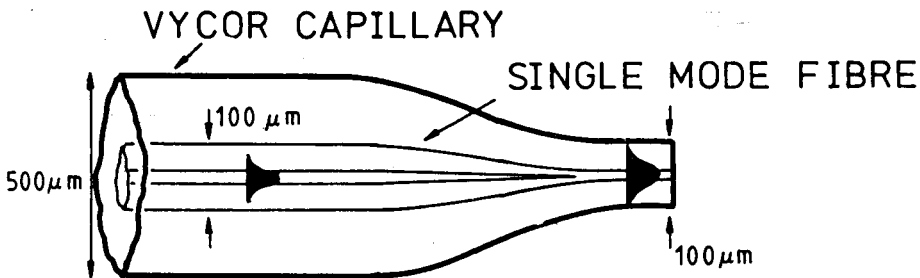


Fig. 5. Taper beam expander with vycor capillary overjacket

FUSED SINGLE MODE FIBRE COUPLERS

(i) Physical Principals and Applications

The fused tapered coupler is the most successful of the single mode couplers, both for stable low-loss operation and ease of fabrication⁶⁻⁸.

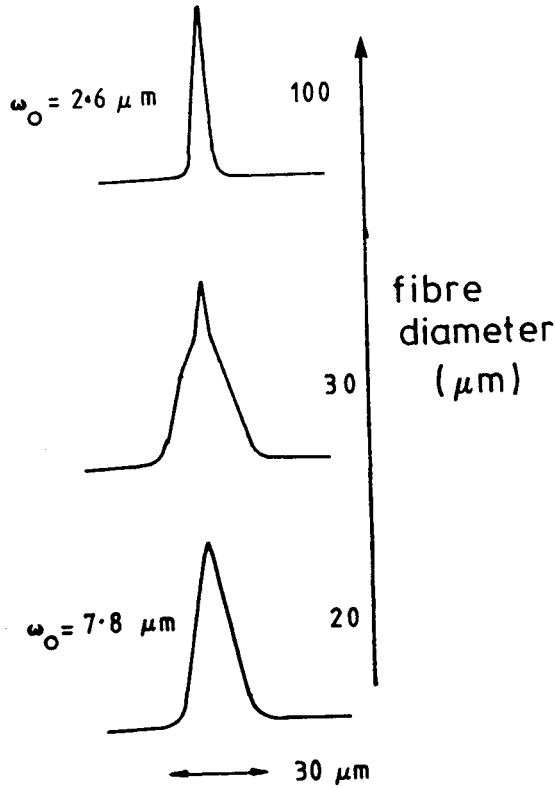


Fig. 6. Field evolution along taper beam expander of Fig. 5.

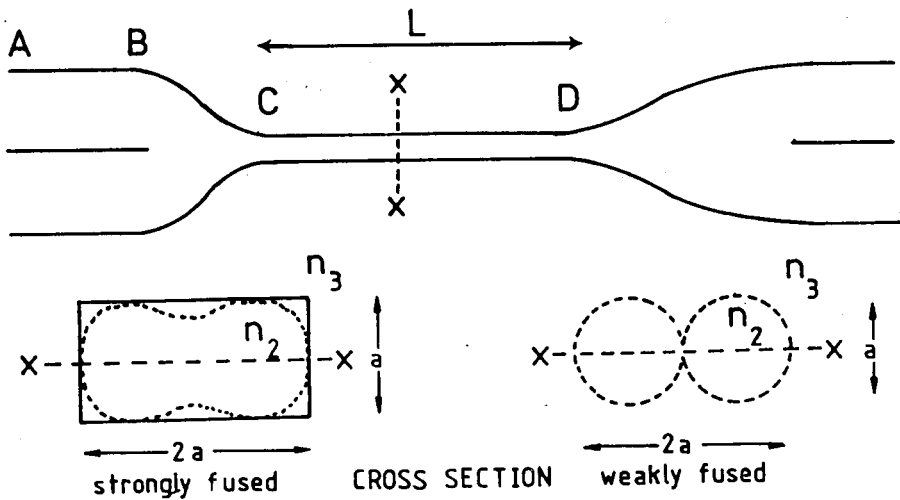


Fig. 7. Fused tapered coupler.

The fused coupler is made by twisting two single-mode fibres together and fusing and pulling to produce a four-port directional coupler, as shown schematically in Fig. 7. The structure of the coupler can be broken down into several elements. Section AB consists of the two input fibres. In section BC the fibres are fused together and tapered adiabatically. Section CD consists of a nearly parallel section where the cross-section has the approximate dumb bell shape shown dotted in Fig. 7. Typical cross sectional dimensions of CD are $10 \times 20 \mu\text{m}$. An optical signal propagating along an input fibre AB will expand as it comes down the taper BC until it becomes a cladding mode. The cladding mode, on reaching the straight

section CD excites the two lowest-order even and odd modes of the composite waveguide whose cross section is shown in Fig 7. From the symmetry of the coupler the power in one of the output ports will be given by

$$P = P_o \cos^2 C \tag{4}$$

The coupling coefficient C is,

$$C = \int_{\text{coupler}} |\beta_e - \beta_o| dz \tag{5}$$

where $\beta_{e,o}$ are the propagation constants of the lowest even and odd modes and the integral is over the entire coupler length. When the fused section of the coupler is long (greater than about 10 mm) the phenomenon of polarisation dephasing is observed^{6,7}. The coupling coefficients for X and Y polarised light are slightly different and are given by

$$C_{x,y} = \int_{\text{coupler}} |\beta_e^{x,y} - \beta_o^{x,y}| dz \tag{6}$$

In a long coupler, with many power interchanges in the fused section, the slight difference in coupling coefficient builds up to result in complete dephasing of the two polarisations, with one polarisation experiencing 100% power transfer at the output and the other none. This results in the modulated response, shown in Fig. 8 for a coupler with a 200 mm fused region, and excited with unpolarised light. The spectral response exhibits a rapid modulation $\Delta\lambda$ due to the large number of power exchanges, and a slower modulation $\delta\lambda$ due to polarisation dephasing. In terms of the coupling coefficients C_x and C_y the spectral response is described by

$$\Delta\lambda = 2\pi \left| \frac{\partial}{\partial \lambda} (C_x + C_y) \right| \tag{7}$$

$$\delta\lambda = \frac{\pi}{2} \left| \frac{\partial}{\partial \lambda} (C_x - C_y) \right| \tag{8}$$

At the modulation minima, described by equation (8), the coupler behaves as a polarisation beam splitter with unpolarised light emerging from the output ports orthogonally polarised.

For shorter couplers polarisation dephasing is not observed and the spectral response is almost sinusoidal⁹ with a period given by (7).

If two couplers with coupling coefficients C_1 and C_2 are concatenated with the throughput port of the first connected to an input port of the second, the combined response at the throughput port of coupler 2 is given by

$$P = P_o \cos^2 C_1 \cos^2 C_2$$

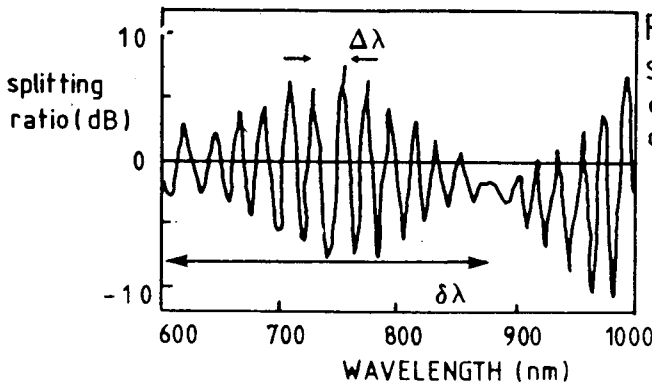


Fig. 8 Spectral response of 200 mm long coupler.

Fig. 8. Spectral response of 200 mm long coupler

If the couplers have different sinusoidal periods then this response is that of a bandpass filter and is the fibre equivalent of the Lyott filter. The calculated response is also shown and close agreement is seen, Fig. 9.

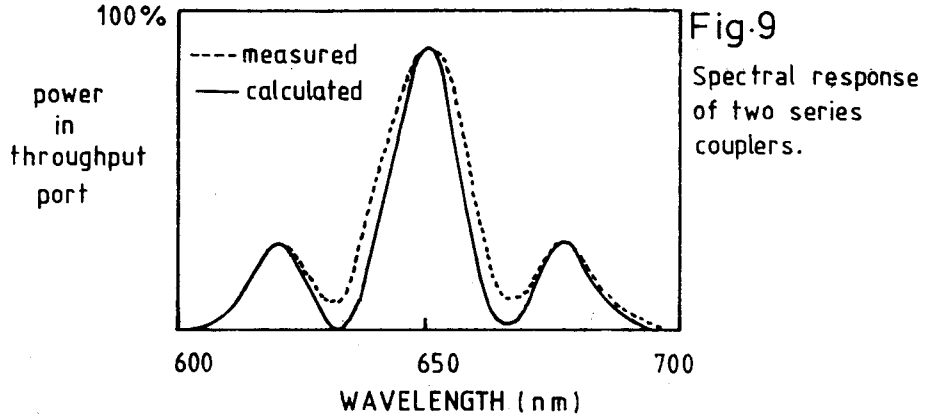


Fig. 9. Spectral response of two series couplers

(ii) Theoretical Analysis

The behaviour of the fused coupler is completely determined once the coupling coefficients C_x, C_y are known. Unfortunately, the integral in equation 5 can only be performed with great difficulty. However, if the fused cladding mode section of the coupler is more than a few mm long we can approximate the coupling coefficient by integrating over the cladding modes only^{11,12}.

$$C = \int_{\text{cladding modes}} |\beta_e - \beta_o| dz$$

For a typical coupler, the cross section of the fused region in Fig. 7 may be as small as $3 \times 6 \mu\text{m}$. The V value of this waveguide is about 30 at $\lambda = 633 \text{ nm}$ in air. At such a high value of V the propagation constants $\beta_{e,o}$ are insensitive to the detailed shape of the cross section, and we can approximate this by a rectangle, as shown in Fig. 7. The rectangular dielectric waveguide, at high V , can be analysed analytically^{11,12}. The following results are then obtained:¹¹⁻¹³

$$C_x + C_y = \frac{3 \pi \lambda}{32 \eta_2 a^2} \left[\frac{1}{(1 + 1/V)^2} + \frac{1}{(1 + (n_3^2/n_2^2 \times 1/V))^2} \right] \tag{9}$$

$$C_x - C_y = \frac{3 \pi \lambda}{16 \eta_2 a^2} \cdot \frac{1}{V} \left(1 - \frac{\eta_3^2}{\eta_2^2} \right) L, \quad V = \frac{2\pi a(\eta_2^2 - \eta_3^2)^{1/2}}{\lambda}$$

We have assumed that the cladding mode waveguide is of constant cross section and length L . Because of the simple analytic form of these equations it is easy to allow for the taper shape. Equation (9) is approximately proportional to λ at high V and this gives a sinusoidal spectral behaviour, as observed. Quantitative agreement with the measured wavelength dependence is very good¹¹⁻¹³ as is the dependence on external refractive index.

Some couplers do not have a strongly fused cross section, but have a cross section approximating to two touching cylinders, Fig. 7. In this weakly fused case the coupling coefficient are given by¹¹.

$$C_x + C_y = \frac{2^{7/2} (\eta_2^2 - \eta_3^2)^{1/2} u_\infty^2}{\eta_2 a \sqrt{\pi} V^{5/2}}$$

$$C_x - C_y = \frac{2^{5/2} (\eta_2^2 - \eta_3^2)^{3/2} u_\infty^2}{\eta_2^3 a \sqrt{\pi} V^{7/2}}, \quad u_\infty \approx 2.405$$

These equations have been tested by analysing the polarisation dephasing in long couplers and in particular it can be shown that

$$\delta\lambda/\Delta\lambda = G \cdot V/(1 - \eta_3^2/\eta_2^2)$$

Where $G = 5/7$ for the weakly fused case and $1/4$ for the strongly fused case. This equation is also in very good agreement with experiment^{11,12}.

In conclusion we have reviewed the physical principles and properties of fused couplers and have presented a detailed theory which provides an accurate description of their behaviour.

REFERENCES

1. D. Marcuse, *Bell Sys. Tech. J.* **56**, 703, (1977).
2. W.J. Stewart and J.D. Love, *ECOC 1985*, 559-562.
3. A.W. Snyder and J.D. Love, "Optical Waveguide Theory", Academic NY, 1983 p. 412.
4. A.R. Beaumont, University of Southampton Final Year Project Report (1984)
5. H. Haus, "Waves and Fields in Optoelectronics", Prentice Hall, (1983).
6. M.S. Yataki, D.N. Payne and M.P. Varnham, *Electron. Lett.*, **21** 249-251 (1985).
7. T. Bricheno and A. Fielding, *Electron. Lett.*, **21** 251-252 (1985).
8. T. Bricheno and A. Fielding, *ibid.*, **20**, 230-232 (1984).
9. F. De Fornel, C.M. Ragdale and R.J. Mears, *IEE Proc. J., Optoelectron.*, **131** 221-228, (1984).
10. M.S. Yataki, D.N. Payne and M.P. Varnham, *Electron. Lett.*, **21**, 248-249 (1985).
11. F.P. Payne, C.D. Hussey and M.S. Yataki, *Electron. Lett.*, **21**, 561-563 (1985).
12. F.P. Payne, C.D. Hussey and M.S. Yataki, *ibid.*, **21**, 461-462 (1985).
13. F.P. Payne, C.D. Hussey and M.S. Yataki, *ECOC 1985*, pp 571-574.